ORIENTAL JOURNAL OF CHEMISTRY
An International Open Access, Peer Reviewed Research Journal
www.orientjchem.org
ISSN: 0970-020 X
CODEN: OJCHEG
2024, Vol. 40, No.(4):
Pg. 1027-1034

Photocatalytic Degradation of Azure-A using Visible Light-responsive Metal Bismuth Iodides: A Comparative Study

SURAJ SHARMA*, JAYANTI L CHAPLOT[1], ADHIDESH S. KUMAWAT[2] and KUMUD INTODIA[3]

[1]A.V college of Arts, K.M College of Commerce and E. S. A College of Science, Vasai Road Dist. Thane, Maharastra, India.
[2]NIT Rourkela, National Institute of Technology, Rourkela, India.
[3]Department of Chemistry, Government Meera Girls College, Udaipur–313001, Rajasthan, *Suraj Sharma-Nathdwara Institute of Biothechnology and Manangement, Nathdwara, Rajsamand Rajsthan, India.
*Corresonding author E-mail: suraj.sharma3059@gmail.com

http://dx.doi.org/10.13005/ojc/400412

(Received: May 10, 2024; Accepted: July 26, 2024)

ABSTRACT

The total annual contribution of textile, material, and other industrial effluents is large in numbers and discharges into water bodies that are not biodegradable. Hence, there is a need for the disposal of dyestuff water effluents with financially savvy innovation. In this regard, photocatalytic degradation of Azure-A is considered a highly significant and acceptable procedure for organic dye decomposition. In the past few years, metal iodide has also received much attention due to its great decomposition efficiency as a photocatalyst to decompose different organic dyes. The present work investigates the comparative photocatalytic competence of synthesized metal bismuth iodides (MBI). The various operational parameters, such as the effect of the Azure-A concentration, the amount of photocatalyst, the pH of the experimental solution, and the intensity of light, were studied. The maximum degradation values for cobalt bismuth iodide were obtained. Photocatalysts were static and maintained significant degradation efficiency, ensuring their reusability.

Keywords: Azure-A, Metal bismuth Iodide, Photo-decomposition, Photocatalyst.

INTRODUCTION

The enormous enlargement of industrialization and urbanization has a terrible impact on water pollution in the last few decades. Therefore, there is a requirement for better sustainable “green technology” that can be advantageous to minimize water pollutants from wastewater. Physico-chemical methods are not suitable due to the usage of various chemicals, which

produce a large amount of sludge. An increse in water quality required an environmentally friendly, more efficient, and more appropriate approach. Recently, photocatalytic degradation of organic dyes has become a significant approach for water purification[1]. This process had several advantages, such as requiring a mild temperature and pressure, complete mineralization, and no need for waste disposal; hence, it is known as "green technology"[2]. In this context, individual consideration depends on heterogeneous photocatalytic degradation of organic dye using Metal Bismuth Iodides. Early studies on photocatalysts only focused on titania (TiO_2)-based photocatalytic degradation induced by UV light[3-5]. However, visible light takes up 43% of total solar radiation, whereas UV light takes up only 4%, Hence, visible light-responsive photocatalysts have gained much attention[6,7].

We emphasize the synthesis of visible light-responsive Metal Bismuth Iodide with significant photodegradation activity and the ability to decompose organic pollutants. Recently, various types of iodides such as A_2MI_4, AMI_3, and A_3MI_5, which are thermochromic materials and exhibit a high value of superionic conductivity within the solid-state have been synthesized[8,9]. $RbPbI_3$ nanostructures with different morphologies have also been synthesized, they posses potential utilization as a light harvester in solar cells[10]. These iodides exhibit good photocatalytic activity and are used to degrade dyes as module pollutants. According to reported literature, Ag_2CdI_4/ZnO[11], Cu_2ZnI_4/Zno[12], Ag_2CdI_4[13], $RbPbI_3$[14] and, y-$CsPbI_3$[15] were used to degrade methyl orange and methylene blue from wastewater.

Various photocatalysts were reported to degrade thiazine dye, such as M/TiO_2 (M=Cu, Ni, Co, Fe, Mn, and Cr)[16], by using biocompatible TiO_2 nanoparticles[17], silver nanoparticles[18], doped ZnS[19], Fe doped ZnS[20], $BiFeO_3$ Nanoparticles[21], and in-doped SnO_2[22]. Sebatini *et al.,*[23] synthesized the α-Fe_2O_3 mesoporous network to degrade thiazine dye. Bharti *et al.,*[24] reported the 80-100% degradation of thiazine dye with the help of Mn-doped TiO_2. Shrivind[25] investigated the degradation of MB and RhB dyes using NiO coupled SnS_2 nanoparticles in the visible range of wavelength.

Thiazine groups containing Azure-A dye can be significantly degraded by metal oxides such as ZnO[26] nanoparticles as repared by the sol-gel process. Experimental results explained that the maximum photodegradation of 89% of Azure-A dyes occurred with a ZnO photocatalyst in an acidic medium.

To the best of our knowledge, the synthesis of Metal Bismuth Iodides by simple Co-precipitation method assistance with solid-state reaction has not been reported. So, in the present study significantly effective and efficient Metal Bismuth Iodide photocatalyst was synthesized by the simple co-precipitation method followed by a solid-state reaction. The Azure-A dye is a basic cationic dye that was used as a module dye pollutant to evaluate its comparative photocatalytic competence over visible-light-induced Metal Bismuth Iodide.

In Fig. 1, Azure-A is an organic dye having fused aromatic rings and an unsaturated structure, and its molecular formula is $C_{14}H_{14}ClN_3S$. It is light blue to dark blue. For the screening of mucopolysaccharides, Azure-A is used as a promising dye. It is often applicable to the lysosome and Giemsa stain.

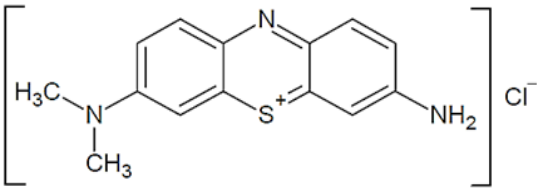

Azure-A

Fig. 1 Structure of Azure-A

The IUPAC name of Azure-A is N', N'-dimethylphenothiazin-5-ium-3,7-diamine chloride. It may also be known as asym-dimethyl-thionine chloride or methylene Azure-A. Its molar mass is 291.8 g/mol. It is a basic dye that belongs to the thiazine group of dyes. Its absorption maxima are at 625–634nm.

EXPERIMENTAL

Chemicals and Experimental Methods

Azure-A dye is purchased in analytical grade. All the materials and chemicals used for synthesis were received from Merck. The XRD (Rigaku Ultima IV X-ray diffractometer using Ni-filtered Cu Ka radiation) and, FESEM pictures

of the catalyst were obtained from the Hitachi-PU 5.0 kV and UV-Vis spectrophotometer Hitachi 330 (Lambda 900, PerkinElmer, Chandigarh). The pH meter (Syntonic, India) and hot air oven were used for maintaining the pH of the experimental solution and drying the prepared photocatalyst, respectively.

Synthesis of Photocatalyst

The Metal Bismuth Iodides nanoparticles were synthesized at a minimum temperature by a co-precipitation technique. Firstly, we prepare Metal Iodides (CoI_2, NiI_2, and CdI_2) and Bismuth Iodides (BiI_3) from their 0.1 mol of respective nitrates and 0.1 mol of KI solution by the co-precipitation method as reported[27,28]. Then, using a solid-state reaction, each Metal Iodides was mix with Bismuth Iodide in a 1:1 mole ratio to obtaine three different Metal Bismuth Iodides. Named Cobalt Bismuth Iodide (CBI), Nickel Bismuth Iodide (NBI), and Cadmium Bismuth Iodide (CdBI). Then they undergo thermal treatment at relatively low temperatures (50-60^{0}C) to remove excess iodine and untreated nitrate. At last, catalysts are allowed to cool themselves naturally outside the oven. The general equation for co-precipitation is as follows:

$$M(NO_3)_x.xH_2O+KI \longrightarrow MI_x(s)+H_2O(l)+KNO_3(aq.) \quad (1)$$

$$Bi(NO_3)_3.5H_2O+KI \longrightarrow BiI_3 \quad (2)$$

$$MI_x+BiI_3 \longrightarrow MBiI_{x+3}\ [M=Co, Ni, Cd] \quad (3)$$

Setup and Degradation Measurement

The degradation experiment was examined at room temperature in a visible region of light (Tungsten lamp = 200 Watt) for 100 minute. After every 10 min, 3 mL of the tested sample was pipped out, and its degradation ability was measured by a visible spectrohotometer at 600nm. At the start of the photodegradation cycle, the samples are placed in the dark region to assess the adsorption capacity of the catalyst for 30 minute. In this procedure, samples contained a fixed 50 mL of Azure-A dye solution with a diverse amount of catalysts (0.06-0.24 g), different contaminant concentrations, and pH limits of 2–10.

RESULT AND DISCUSSION

Characterization

XRD analysis

Figure 2 gives the combined XRD peaks of Metal Bismuth Iodides which show great agreement with other simulated data mentioned in the previous literature. Each photocatalyst possesses a highly crystalline nature according to most intence diffraction peaks at 2 theta value. The partical size is evaluated by applying the Scherrer equation:[29]

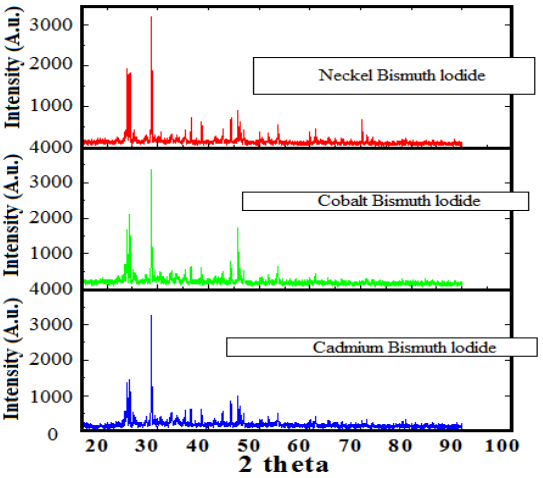

Fig. 2. XRD Pattern of CBI, NBI, and CdBI

$$D = \frac{0.9\lambda}{\beta \cos\theta}$$

Where "D" is the crystallite size, λ is the wavelength of X-rays, θ is the Bragg diffraction angle, and β is the full width at half maximum of the diffraction peak.

At different 2 theta values, we obtained the calculated approximate crystallite size of the prepared photocatalyst as 59nm, 61nm, and 50nm of compound Cobalt, Nickel, and Cadmium Bismuth Iodide respectively.

FESEM and EDAX Analysis

Figure 3 shows FESEM images of Cobalt, Nickel, and Cadmium Bismuth Iodide prepared at comparatively low temperatures. As observed in Fig. 3(a), Cobalt Bismuth Iodide posses a sheet-like structure and tiny particles. Fig. 3(b) shows the tetragon plate with circular corners of Nickel Bismuth Iodide while Fig. 3(c) pretends to be a sheet-like structure on which tiny particles of cadmium are distributed uniformly. The chemical precision of as-prepared photocatalysts is explored by electron diffraction X-ray spectroscopy (EDX). In Fig. 4 (a-c), it is visible that the product has Co, Ni, Cd, Bi, and I. The EDS spectrum appears to have no extra irrelevent peaks, which confirm the purity of product.

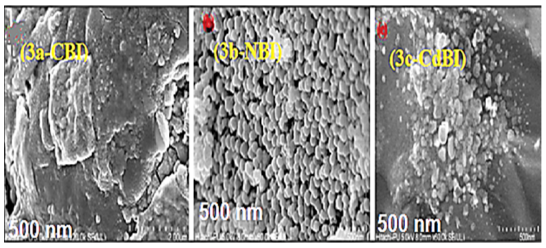

Fig. 3(a-c). FESEM Image at Different Magnification

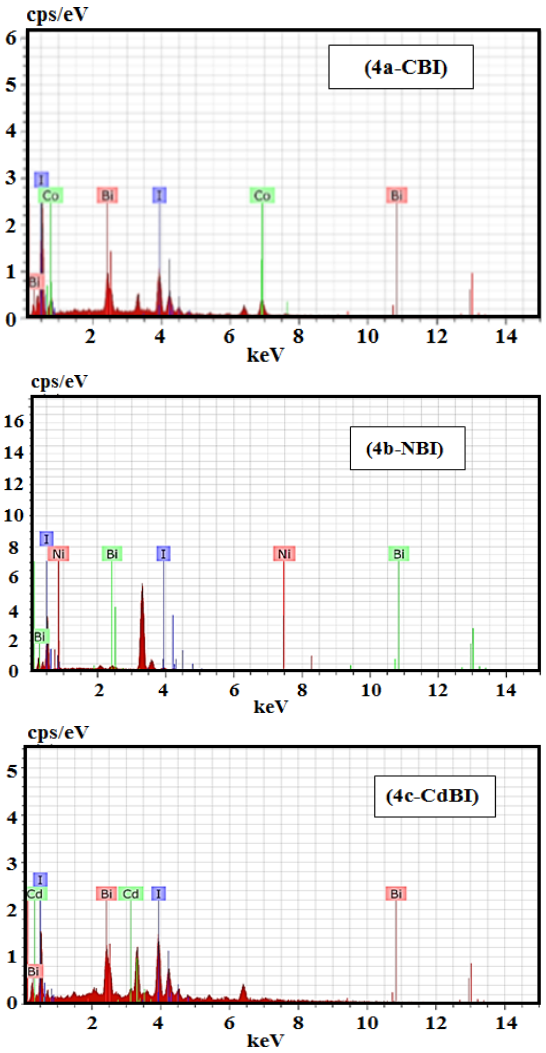

Fig. 4(a-c). EDX spectra of (a) CBI (b) NBI (c) CdBI

Photocatalytic Efficiency of Metal Bismuth Iodides

The characteristic absorption maxima for Azure-A lie at the wavelength of 600nm, which has been utilized to illustrate the photocatalytic degradation reaction. Fig. 5 represents the photodegradation percentage of Azure-A as a function of illumination time without a photocatalyst and over CBI, NBI, and CdBI. The photodecomposition rate of the Azure-A dye was determined using the following equation:

$$D = \left[1 - \frac{Af}{A_i}\right] x\ 100 \qquad (5)$$

Here, D is the percentage dye degradation, Af is the final absorption of Azure-A at the wavelength 600nm, and Ai is the initial absorption of Azure-A. It was concluded that the photodegradation of Azure-A under visible light without any photocatalyst was neglectable (Fig. 5d). Azure-A was showing almost complete degradation after 100 min of exposure under visible light by CBI (Fig. 5a) and CdBi (Fig. 5b). However, only 50 min of visible light exposure can degrade Azure-A dye by NBI (Fig. 5c). The degradation of Azure-A using photocatalyst was fitted for pseudo-first-order kinetics, and the efficiency of decomposition of Azure-A can be achieved by applying the following expression:

$$k = 2.303 \times \text{slope} \qquad (6)$$

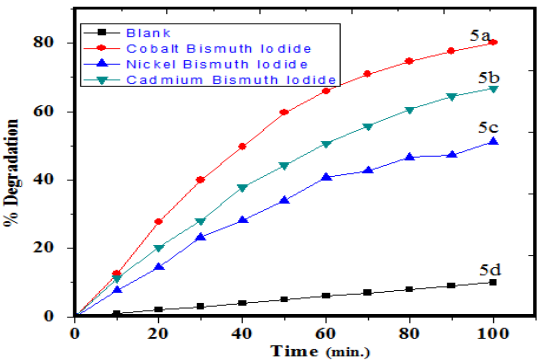

Fig. 5. Azure-A degradation by Metal Bismuth Iodides

Calculated k values for the CBI, NBI, and CdBI were 2.68, 2.30, and 1.92x10^{-4} s^{-1} respectively. The CBI exhibits higher photocatalytic efficiency compared to other catalysts. The decreasing order of the rate of reaction for the photocatalytic decomposition of Azure-A dye was obtained as:

The optimum condition for all three MBIs were mentioned in the following Table 1.

Impact of Involved Parameters

In the presented experimental work, the investigation was done to analyze the impact of the four most examined parameters on degradation effeciency of Azure-A such as- the amount of catalyst, pH, Azure-A concentration, and intensity of light irradiation.

Table 1: The optimum condition for all three MBI

Sr. No	Photocatalyst	Concentration(mM)	pH	Catalyst Dose (g)	Light Intensity(mW/cm²)	Rate of Reaction(kx10⁻⁴)
1	CBI	85	8	0.20	70	2.68
2	NBI	70	6	0.14	70	2.30
3	CdBI	70	9	0.18	70	1.92

Impact of pH on Degradation Activity

The first operational factor in the experiment is the pH of the model pollutant; this is due to its charge density thickness outside the particles of the examined dye as well as the imerged prepared catalyst in solution. Therefore, the impact of pH on degradation Azure-A competence was analysis to ascertain the extent to which the pH of the solution may affect the decomposition speed. This step was done by utilizing 50 mL of Azure-A dye solution and a 0.10 g catalyst, varying the solution pH values from 2 to 10. The various trends of Azure-A degradation at different pH values are represented in Fig. 6(a-c). The obtained outcome from the graph shows that the decomposition capacity of Azure-A was influenced by the pH of the solution. At higher pH, the higher decomposition tendency could be associated with the influence on the pH of the experimental sample, which is also applicable for photocatalyst surfaces. In the high pH region, there is a higher number of protons present in the experimental solution. The area of the photocatalyst gets positively charged, especially below 5 pH; and this positively charged catalyst molecule is not providing the OH groups required for radical generation. Azure-A was also acidified at a lower pH. It reduces the ability of cation-pi binding among metals and Azure-A; hence, there was repulsion between catalyst and dye particles. All mentioned reasons for the less photo-decomposition ability examined at lower pH. However, as pH values increase, the photocatalyst (CBI, NBI and CdBI) surface becomes progressively deprotonated, while the Azure-A also gets uncharged and less charged. As a result, there was increased contact or adsorption between the photocatalyst and Azure-A. Moreover, deprotonations result in the discharge of OH ions, which respond to electron holes to generate OH. free radicals, which improve the rate of Azure-A decomposition. The intensifiation of adsorption and the increment of hydroxyl radical generation sped up the Azure-A degradation efficiency at pH 8 (CBI), 6 (NBI), and 9 (CdBI) in comparison to lower pHs. Hence, the pH of the reaction mixture had a great impact on the ionization of the sample in the dye solution, which obviously governs the dye degradation activity.

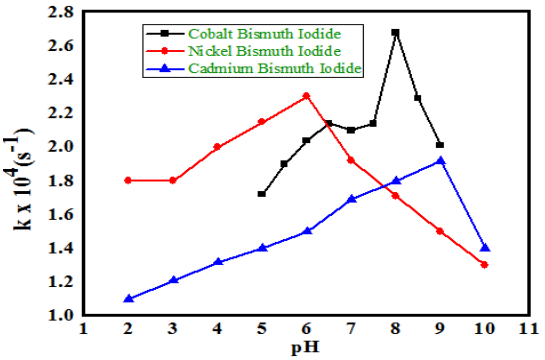

Fig. 6. Impact of pH on Dye Degradation

Effect of Metal Bismuth Iodides dose

The effect of the dose of MBI on the Azure-A decomposition competence is monitored to obtain the maximum dose of photocatalyst needed for photodegradation of a fixed concentration of Azure-A in a fixed volume of experimental sample. Therefore, the observation is being executed by taking 50 mL of Azure-A solution with a different amount of photocatalyst (0.06 g to 0.24 g). The obtained outcomes of observation are represented in Fig. 7. Experimental details explained that the manifold photocatalysts and their diverse amounts show good effects on the Azure-A decomposition. These consequences of the shown data may be described as follows; At the optimum amount of photocatalyst, there was proper equilibrium between the exposed photocatalyst surfaces and the penetrating UV light pathlength. This encourages the elevated formation of negative and positive pairs of ions that stimulate the generation of a number of hydroxyl radicals. These transform radicals were responsible and considered the main species for the Azure-A photo-decomposition procedure. However, after the corresponding values (CBI=0.20 g), (NBI=0.14 g), and (CdBI=0.18 g), the solution opaqueness increased due to a cluster of catalysts in the reaction mixture. So, the amount of penetrating photon gets decreased and becomes unavailable to reach the catalyst surface. As a result, fewer electron holes are generated and a smaller amount of OH. radicals are stimulated. Thus, the rate of degradation observed increasing as loading increased is logical until the maximum level.

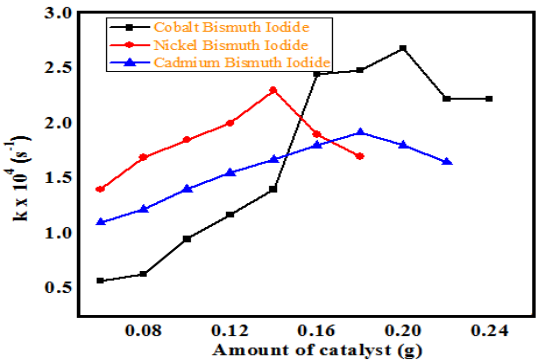

Fig. 7. Impact of Catalyst Loading on Dye Degradation

Impact of Azure-A Dye Concentration on Decomposition Efficiency

The competence of Azure-A decomposition and removal was superiorly governed by various concentrations of monitored dye solutions. The experimental sample solution and the active catalyst surface are both responsible for influencing the degradation rate. In this work, the impact of the introductory dye concentration on the degradation rate of the taken samples was analyzed by spectrophotometer. The Azure-A model dye concentration was varied from 55 mM to 95 mM The obtained comparative result of Metal Bismuth Iodides were mentioned in Fig. 8 reveals that the degradation efficiency of Metal Bismuth Iodides was found to relatively increase with a variety of initial dye concentrations until a certain value. After this, degradation efficiencies were a decreasing trend with an increase in dye concentration. This trend appears due to the adsorption area of the synthesized Metal Bismuth Iodides in all the samples. CBI showed a superior efficien cy of 80% at an initial dye concentration of 85-mM.

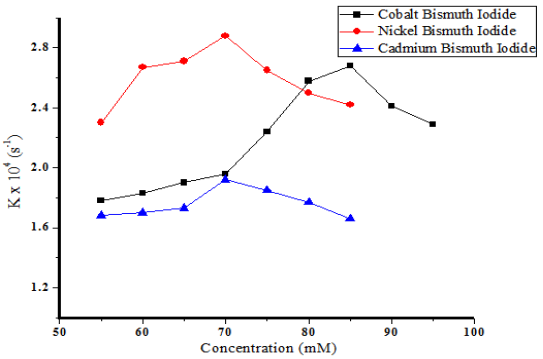

Fig. 8. Impact of Azure-A dye Concentration

Impact of Light Intensity on Degradation Efficiency

The effect of visible light intensities on the efficacy of photocatalytic Azure-A decomposition using CBI, NBI, and CdBI was shown in Fig. 9. The represented result explained that increasing the light intensity until it reaches its maximum value increased the efficacy of the dye system. This is due to the on increasing the visible light intensity also increases the number of photons received by the photocatalyst, which increases electron stimulation and, in turn, enhances system degradation efficacy. The eviction of organic dyes observed that the degradation efficacy of the polluted dye model was elevated by enhancing the light-intensity and illumination time, which was in accordance with the concent obtained for the present study.

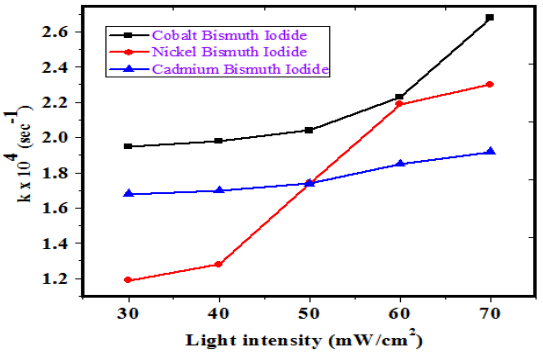

Fig. 9. Impact of Light Intensity on Dye Degradation

Mechanism

The photocatalytic mechanism of Azure-A with the as prepared Metal Bismuth Iodide (MBI) has been proposed. In a typical photocatalytic process, the light of the appropriate wavelength is absorbed by the dye, which then gets excited to its first singlet state, which further follows intersystem crossing to get its triplet state. Photocatalyst Metal Bismuth Iodide will absorb light of a suitable wavelength and then conduct a light quantum attack on the catalyst (MBI) surface, which will excited the electrons of the valence band (VB) towards the conduction band (CB) and create an electron-hole pair. O_2 present in water will react with electrons present in CB, whereas the newly formed VB hole will react with water molecules on the MBI surface to create •OH radicals. •OH radical may behave like a functioning oxidizing species, which then oxidizes the Azure-A to its leuco structure, which breaking down the Azure-A into a less poisonous substance. The reactions could be summarized in the following manner:

$^1AA_0 \longrightarrow {}^1AA_1$ (Singlet excited state)

$^1AA_1$ (Singlet excited state) $\longrightarrow {}^3AA_1$ (Triplet State)

$MBI \longrightarrow [e^- (CB)+h + (VB)]$

$h^+ + {}^-OH \longrightarrow$ •OH (oxidation)

$H_2O + h^+ \longrightarrow H^+ + \bullet OH$

$e^- + O_2 \longrightarrow O_2.^-$(Reduction)

$O_2\bullet^- + HO\bullet_2 + H^+ \longrightarrow H_2O_2 + O_2$

$\bullet OH + {}^3AA_1 \longrightarrow$ (Leuco) AA

Leuco AA $\longrightarrow$ Products

Durability and Recyclability

The feasibility, durability, and reusability of all photocatalysts are the most crucial factors for their commercial and extensive uses. Therefore, MBI catalyst was obtained after every experimental cycle and washed with 15 mL of a 50% ethanol solution, dried at 50°C in a hot air oven, and utilized in the next experimental cycle. In Fig. 10 the significance of the decomposition of MBI became stable during each run. These MBI can be utilized as a recoverable and economically beneficial catalyst for the decomposition of Azure-A.

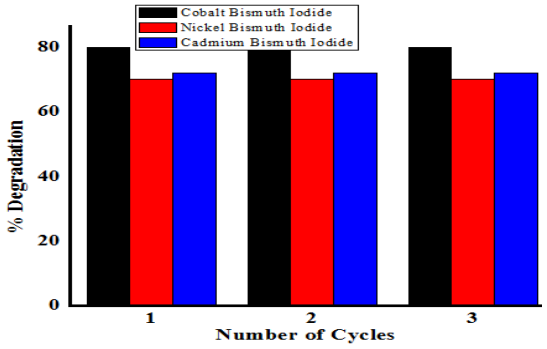

Fig. 10. Stability and Re-usability

CONCLUSION

Visible light-induced MBI with a size ranging from approximately 50nm to 61nm was synthesized by a co-precipitation and solid-state reactions. The utilized Azure-A solution in experiments (50 mL) was degraded 80% in 100 min over the CBI photocatalyst under visible light illumination, which was higher than that over the NBI and CdBI. These photocatalysts were most effective at higher concentrations than lower concentrations. They have also exhibited higher degradation of Azure-A in alkaline mediums with an inferior amount of catalyst loading. All of them possess good stability and durability over the 3 successive cycles.

ACKNOWLEDGMENT

We are enormously thankful to the staff members of the department of chemistry at Government Meera Girls College, Udaipur, for their combined efforts in experimental work.

Conflict of Interest

The authors proclaim that there are no affiliations with or contributions in any association or substance with any monetary interest or non-monetary interest in the topic or materials talked about in this manuscript.

REFERENCES

1. Rafiq, A.; Ikram, M.; Ali, S.; Niaz, F.; Khan, M.; Khan,Q.; Maqbool, M., *J. Ind. Eng. Chem.*, **2021**, *97*, 111-128.
2. Cao, Y.; Zhou, G.; Zhou, R.; Wang, C.; Chi, B.; Wang, Y.; Hua, C.; Qiu, J.; Jin, Y.; Wu, S., *Sci. Total Environ.*, **2020**, *708*, 134669.
3. Madkhali, N.; Prasad, C.; Malkappa, K.; Choi, H. Y.; Govinda, V.; Bahadur, I.; Abumousa, R.A., *Results Eng.*, **2023**, *17*, 100920.
4. Xu, D.; Yu, H.; Qin, Y.; Di, Y.; Jia, H.; Li, H.; Liu., *J.Appl. Nano. Mater.*, **2024**, *7*, 2630-2638.
5. Miao, B.; Asad, M.; Zhang, Y.; Chen, Q.; Zhang, M.; Bia, Z.; Zhao, Y.; Lin, G., *J. Alloys. Compd.*, **2024**, *976*, 173362.
6. Yangjeh, A. H.; Feizpoor, S.; Seifzadeh, D., *Sep. Prif. Technol.*, **2020**, *238*, 116404.
7. Hu, X.; Sun, Z.; Son, J.; Zhang, G.; Li, C.; Zheng, S., *J. Coll. Interf. Sci.*, **2019**, *533*, 238-250.
8. Wang, Z.B.; Zhang, Y.H.; Sun, Y.L.; Lv, M.H.; Liu, Y.; Li, W.Z.; Luan, J.; Zhang, X.S., *J. Mater. Chem.* C., **2024**, *9*, 3011-3325.
9. Xu, L.; Wang, P.K.; Jiang, Z.; Yu, J. C., *Appl. Catal. B Environ.*, **2023**, *338*, 13080.
10. Ahmad, A., *Bull. Mater. Sci.*, **2010**, *33*, 419-425.
11. Ghanbari, M.; Soofivand, F.; Nisarri, M. S., *J. Mol. Liq.*, **2016**, *223*, 21-28.
12. Razi, F.; Soofivand, F.; Nisarri, M. S., *J. Mol. Liq.*, **2016**, *222*, 435-440.
13. Ghanbari, M.; Gholamrezaei, S.; Niasari, M. S.; Abbasi, A., *J. Mater. Sci. Mater. Electron.*, **2017**, *28*, 6272-6277.
14. Ghanbari, M.; Sabet, M.; Niasari, M. S., *J. Mater. Sci. Mater. Electron.*, **2016**, *27*, 8826-8832.
15. Zhang, Q.; Tai, M.; Zhou, Y.; Zhou, Y.; Wei, Y.; Tan, C.; Wu, Z.; Li, J.; Lin, H., *ACS Sustainable Chem. Eng.*, **2020**, *8*, 1219-1229.

16. Kuyumai, O. K.; Kibar, E.; Dayioglu, K.; Gedik, F.; Akin, A. N.; Aydinoglu, S. O., *J. Photochem. Photobiol. A Chem.*, **2015**, *311*, 176-185.
17. Bharti, B.; Sonkar, A. K.; Singh, N.; Dash, D.; Rath, C., *Mater. Res.*, **2017**, *4*, 085503.
18. Joseph, S.; Mathew, B., *J. Mol. Liq.*, **2015**, *204*, 184-191.
19. Chauhan, R.; Kumar, A.; Chaudhary, R. P., *J. Lumin.*, **2014**, *145*, 6-12.
20. Chauhan, R.; Kumar, A.; Chaudhary, R. P.; *Spevtrochim. Acta* A., **2013**, *113*, 250-256.
21. Azmy, H. A. M.; Razuki, N. A.; Aziz, A. W.; Sator, N. S. A.; Kaus, N. H. M., *J. Phy. Sci.*, **2017**, *28*, 85-103.
22. Zeferino, R. S.; Pal, U., *Adv. Nano. Res.*, **2019**, *7*, 13-24.
23. Sabatini, S.; Kalluri, S.; Madhavan, A. A., *Mater. Latt.*, **2020**, *5*, 100037.
24. Bharati, B.; Mishra, N. C.; Sinha, A. S. K.; Rath, C., *Mater. Res. Bull.*, **2020**, *123*, 11010.
25. Srivind, J.; Nagarethinam, V. S.; Suganya, M.; Balamurugan, S.; Usharani, K.; Balu, A. R., *Vaccum.*, **2019**, *163*, 373-378.
26. Hussain, B. S.; Waheeb, A. S.; Yasir, A. M.; Alshams, H. A., *J. Phy. Conf. Ser.*, **2019**, *1294*, 052048.
27. Sharma, S.; Samota, J.; Bhardwaj, S.; Intodia, K., *Orient. J. Chem.*, **2020**, *36*, 286-292.
28. Sharma, S.; Samota, J.; Bhardwaj, S.; Intodia, K., *Poll. Res.*, **2020**, *39*, 1175-1179.
29. Fatimah, S.; Ragadhita, R.; Husaeni, D F A.; Nandiyanto, A B D., *Asian. J. Sci, Eng.*, **2022**, *2*, 65-76.